Biotechnology Reports 30 (2021) e00638

Contents lists available at ScienceDirect

Biotechnology Reports

journal homepage: www.elsevier.com/locate/btre

Oily water treatment in a multistage tower operated under a novel induced pre-saturation process in the presence of a biosurfactant as collector

Leonardo Bandeira dos Santos[a,b,*], Rita de Cássia Freire Soares da Silva[a,c], Pedro Pinto Ferreira Brasileiro[a,d], Rodrigo Dias Baldo[e], Leonie Asfora Sarubbo[a,b,c], Valdemir A. dos Santos[a,b,c]

[a] Advanced Institute of Technology and Innovation (IATI), Potira 31, Prado, 50751-310, Recife, Pernambuco, Brazil
[b] Northeast Biotechnology Network, Federal Rural University of Pernambuco, Rua Manoel de Medeiros, s/n, Dois Irmãos, 52171-900, Recife, Pernambuco, Brazil
[c] Centre for Sciences and Technology, Catholic University of Pernambuco, Rua do Príncipe, n. 526, Boa Vista, 50050-900, Recife, Pernambuco, Brazil
[d] Department of Chemical Engineering, Federal University of Pernambuco, Av. dos Economistas, s/n, CEP 50740-590, Recife, Brazil
[e] Centrais Elétricas da Paraíba – EPASA, Brazil

ARTICLE INFO

Article history:
Received 31 October 2020
Received in revised form 22 May 2021
Accepted 24 May 2021

Keywords:
Oily water
Biosurfactant
Liquid-liquid separation
Operation diagram
Bench prototype

ABSTRACT

The increase in water-oil separation efficiency as a function of biosurfactant in a novel process of a continuous induced pre-saturation tower (IPST) with stages was described. The pre-saturation of the effluent in a new IPST prior to its entrance in each stage enabled enhancing the effect of the biosurfactant on the flocculation of oil droplets due to the close contact with the air during the formation of microbubbles inside a centrifuge pump. This change of a conventional dissolved-air flotation device enabled each stage to serve as a final flocculation chamber and flotation separator. The initial flocculation step occurred nearly entirely within the centrifugation pump adapted for the generation of microbubbles. Experimental tests in a bench-scale prototype of an IPST enabled drafting two operation diagrams based on the absence and presence of the biosurfactant produced by the bacterium *Pseudomonas cepacia* CCT 6659. We used an effluent composed of water and semi-synthetic motor oil at 500 ± 13 mg L^{-1}. The oil removal efficiency was estimated with the aid of Damköhler numbers applied under the analogy of considering the IPST to be a set of perfect-mixture tanks in series. To quantify the increase in efficiency achieved with the addition of the biosurfactant, we identified the kinetic laws corresponding to the addition and non-addition of the biosurfactant. The addition of the biosurfactant led to an increase in the oil removal rate in the IPST from 92.5 % to 97.0 %.

1. Introduction

Oils and fats are common industrial pollutants, the removal of which is normally achieved through gravitational separation, such as decantation, centrifugation, flotation, etc. Complex processes requiring high investments have been adopted and minimizing the costs of classic processes seems to be a challenge for many researchers. Therefore, important contributions have been made to technologies aimed at improving classic processes, such as flotation [1].

Due to its operating simplicity, dissolved-air flotation (DAF) has received particular attention from researchers in the field of oily water treatment. A preferential coalescence-adsorption process was recently developed using a cyclonic flotation column in a single structure for the separation of oil from water [2]. This flotation column is fed from the top. A flow of air microbubbles and coal particles adsorb to the oil droplets in the upper portion of the column. Although a relative increase is the oil removal rate is achieved by the combination of the two processes, the additional component of coal particles may give rise to an effluent that requires new separation methods.

Researchers have dedicated efforts toward the implementation of more efficient flotation equipment, such as column flotation cells. However, such equipment does not seem to meet the expectations of enhancing separation efficiency in relation to the

* Corresponding author.
E-mail address: valdemir.alexandre@iati.org.br (L. Bandeira dos Santos).

https://doi.org/10.1016/j.btre.2021.e00638

physical space occupied. The increase in contact time due to the increase in column length does not mean greater efficiency [3]. Turning to the aid of special collectors has also been a common practice in the quest for better performance for DAF devices. However, this strategy requires a large physical structure for the required mixing conditions and contact time. In other words, obedience to a given kinetic law should allow analogies that transform a simple column into a set of separating chambers. Based on this premise and the physical arrangement used in distillation columns, such physical conditions were reproduced in the present study as a way to adjust separation conditions in flotation equipment.

Biosurfactants are compounds obtained from microorganisms that are capable of altering the surface and interfacial properties of liquids. These natural products are biodegradable biodetergents with numerous industrial applications, especially in processes that involve petroleum products, such as the treatment of oil-contaminated soil, the treatment of oily water as well as the cleaning of heavy oil from pipes and storage tanks [4].

To investigate the use of a biosurfactant in the field, it is necessary to perform tests in laboratory prototypes with similar operational characteristics as those used on a pilot scale [5]. Such prototypes must ensure the adequate prediction of the effect caused by the addition of these alternative collectors in situations that simulate difficulties found on a larger scale.

In this work, the action of a biosurfactant was tested in a bench-scale of a new induced pre-saturation (IPST) with different stages. While an IPST performs better than conventional flotation devices, the prototype was used with the biosurfactant to investigate a possible further increase in the removal of oil from water.

2. Materials and methods

2.1. Experimental design

An induced saturation tower with different stages has the same function as DAF column equipment but with modifications and adjustments to the steps of the process. Such modifications enable a reduction in the physical space occupied by the flotation chambers in comparison to conventional DAF [6]. The arrangement in different stages, as occurs in a distillation column, gives an IPST the format shown in the schematic displayed in Fig. 1. The pre-saturation of the effluent with atmospheric air microbubbles is achieved with the aid of a centrifuge pump adapted to generate microbubbles without the aid of a compressor or saturation tank [7].

In an IPST, the saturation stages of the water-oil mixture and the onset of floc formation with or without the addition of an auxiliary collector, such as a biosurfactant, are performed simultaneously during the passage of this mixture through the microbubble pump. Air and the effluent to be treated enter the aspiration line of the centrifuge pump, completing pre-saturation within the discharge line of the microbubble generation pump [8].

The chambers of the IPST are cylindrical and have a conical base. In each stage, the affluent flow containing the liquid saturated with air microbubbles is fed through the top and dispersed at half the height from the base. Within the stage or flocculation-separation chamber, the oil droplets are submitted to flotation, creating an oily foam that rises to the upper portion of the chamber. This foam is removed through an upper outlet located on the side of the lid of the chamber connected to a pipe. This occurs simultaneously in all stages. The outlet was strategically designed to serve as a convergent-divergent diffusor through the shape of the lid of the chamber to facilitate the removal of the oily foam [9]. Moreover, a hydraulic seal maintains the level of the liquid constant in the interior of the stage, enabling the removal of

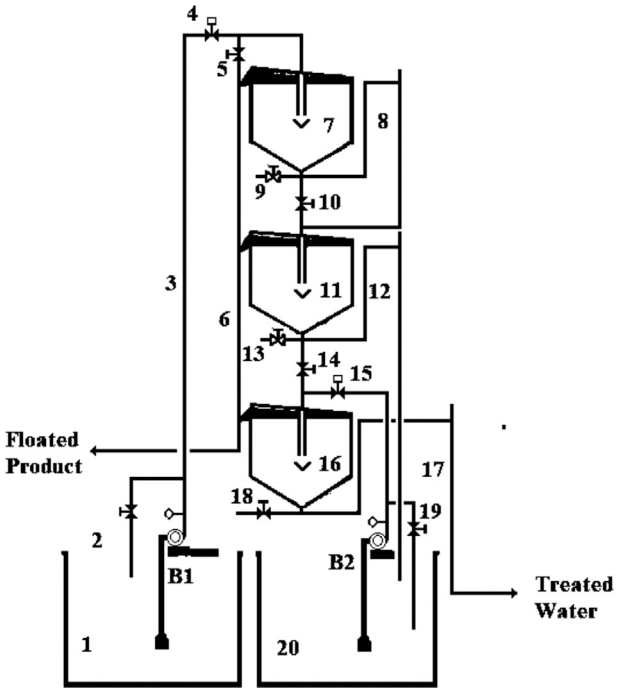

Fig. 1. Schematic of main components of bench-scale prototype of induced pre-saturation tower with different stages. 1 – Feed tank of upper stage; 2 – return valve of Pump 1; 3 – discharge line for Pump 1; 4 – microbubble flow control valve of Pump 1; 5 – flow valve for oily foam suction tube; 6 – oily foam collection pipe; 7 – flotation chamber of upper stage; 8 – hydraulic seal of upper stage; 9 – sample collection valve of upper stage; 10 – discharge valve of upper stage; 11 – flotation chamber of intermediate stage; 12 – hydraulic seal of intermediate stage; 13 – sample collection valve of intermediate stage; 14 – discharge valve of intermediate stage; 15 – microbubble flow control valve of Pump 2; 16 – lower flotation chamber; 17 – hydraulic seal of lower flotation chamber; 18 – sample collection valve of lower flotation chamber; 19 – valve of return pipe of Pump 2; 20 – feed tank of lower stage.

samples from the lower outlet of the stage and the feeding of the following stage. The degree of saturation of this effluent in each stage can be recomposed with an additional saturation before the liquid is sent to the next stage.

The treated water that exits each stage of the IPST has a level of residual oil that depends on the number of stages through which it has already gone (the spatial time to which it was submitted) [10]. The second type of effluent of each stage is an oily foam formed on the surface of the separation-flocculation chamber. The shape of the lip causes a gradual reduction in the physical space for the outflow of the oily foam, which should not accumulate at the top of the chamber. Thus, the foam on the surface of the chamber is aspirated toward the opening on the upper side of the lid. At the base of the tower, water treated in the final stage is collected in a treated-water tank.

2.2. Material for construction of induced saturation tower

When working with the experimental development of equipment, it is advisable to develop prototypes on different scales, which will undergo transformations as the functional characteristics are defined [11]. Thus, one works with materials that are easy to handle but difficult to adapt to certain practical situations, such as high resistance to mechanical forces and high temperatures. For instance, constructing prototypes with transparent materials (glass, acrylic or polycarbonate) gives rise to physical models denominated *cold models* [12,7,13,14]. Such materials enable visualizing important fluid dynamics [15] but also have leakage problems, cracks, low tolerance to high temperatures and other limitations. However, cold models enable modifications within a

short observation period, whereas metal models require long periods of time for the implementation of the necessary corrections.

The stages of the bench-scale TSPI prototype used in this study were constructed in transparent acrylic, PVC, acrylonitrile butadiene styrene (ABS) and aluminum, the latter of which was used as the framework. The lids of the chambers had a more complex shape that the other components and were made in ABS with the aid of a 3D printer [16]. The pipes were made of PVC. The microbubble pumps were centrifuge pumps equipped with devices to eliminate the occurrence of cavitation during the operation of the tower [17]. The pumps should have manometric heights for the elevation of the water column a minimum of 50 m to enable the operation of the tower under conditions greater than those recommended by Han et al. [18] for the generation of microbubbles.

2.3. Control of IPST

The automation and control system for the IPST continuous prototype was designed based on simple strategies according to Galdino et al. [19]. The microbubble generation system consisted of a tank and duly adapted centrifuge pump. The flow of the saturated affluent to the chamber was controlled by a valve to adjust the pressure of the discharge line of the pump, which is necessary for adequate microbubble flow.

The level of the liquid in the chambers was limited by a liquid column that forms a hydraulic seal at a height near the upper side outlet. This outlet only allows the exiting of the oily foam while retaining the purely liquid phase. A second strategy for assisting in the removal of the foam (also shown in Fig. 2) was the placement of a tube with bleeding of the affluent to assist in drawing the oily foam [20]. To avoid the formation of low-pressure zones and the consequent disturbance of the flow through the flotation chamber, the tubing had an additional piece serving as a vacuum breaker [21].

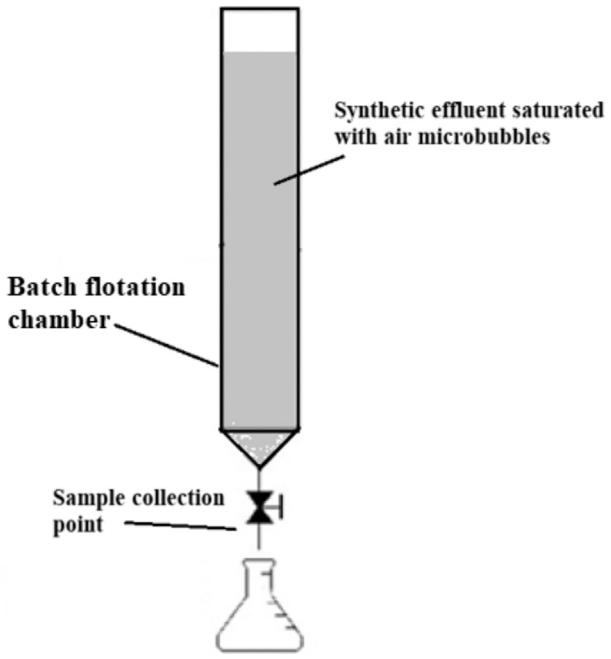

Fig. 2. Experimental batch arrangement for determination of kinetic flotation laws with and without addition of biosurfactant.

2.4. Preparation of biosurfactant

2.4.1. Bacteria and culture

The biosurfactant used in the experiments was produced by the bacterium *Pseudomonas cepacia* CCT 6659, which was acquired from the culture bank of the André Tosello Research and Technology Foundation (Campinas, SP, Brazil). Young cultures of the bacteria were transferred to an Erlenmeyer flask containing 50 mL of brain heart infusion (BHI) and kept under stirring at 150 rpm for 12 h at 28 °C to obtain an optical density of 0.7 (corresponding to an inoculum of 10^7 colony-forming units/mL) at 600 nm.

The culture medium specified by Soares da Silva et al. [22] was used (gL^{-1}): 0.5 of KH_2PO_4, 1.0 of K_2HPO_4, 0.5 of $MgSO_4.7H_2O$, 0.1 of KCl, 0.01 of $FeSO_4.7H_2O$, supplemented with 2.0 % waste canola frying oil and 3.0 % corn steep liquor. The initial pH was adjusted to 7.0. The culture was performed with an inoculum of 1.5 % with stirring at 250 rpm for 60 h at 28 °C.

2.4.2. Determination of surface tension

The surface tension of the liquid was measured at 25 °C using Sigma 700 tensiometer (KSV Instruments Ltd., Helsinki, Finland) equipped with a du Noüy ring [12]. The tension of the surfactant solutions was calculated using the Langmuir method Langmuir [23]: $\gamma_0 = \gamma\ (n/n_0)$, in which γ_0 and γ are respectively the surface tensions of the reference solvent ($\gamma_0 = 73.49$ dyn/cm^2 for water) and surfactant solution and n_0 and n are respectively the number of drops of the reference solvent and surfactant solution.

2.4.3. Biosurfactant purification and isolation

For the isolation of the biosurfactant, the cells were removed from the culture medium after fermentation by centrifugation at 5000 rpm for 30 min. The pH of the filtered supernatant was adjusted to 2.0 with HC1 6.0 M and the addition of an equal volume of $CHCl_3/CH_3OH$ (2:1, v/v). The mixture was shaken vigorously for 15 min and set to rest for the separation of the phases. The organic phase was removed and the operation was repeated three times. The organic phase was concentrated using a rotary evaporator. A viscous yellowish product was obtained, dissolved in methanol and concentrated again by evaporation of the solvent at 45 °C [24]. After extraction, the product was treated with a base and crystallized for the maximal removal of impurities.

2.5. Kinetic models for oil removal

The synthetic effluent used in the experiments consisted of water with motor oil (500 ± 13) mg L^{-1}. The motor oil was semi-synthetic (Shell HELIX-HX6, 15W-40) for use in flex engines. The homogenization of the oil in the effluent was achieved using the procedures described by Rocha e Silva et al. [24]. The emulsion containing the water and motor oil was stabilized with .05 % sodium chlorite (NaCl) and 0.0025 % sodium lauryl sulfate (SLS). The effluent with biosurfactant contained the same components with the same concentrations plus the biosurfactant (0.25 %) from *Pseudomonas cepacia* CCT 6659. Both synthetic effluents were prepared using a vortex shaker at 2800 rpm for approximately ten minutes.

The oil content in the samples was determined using a spectrophotometer following the methods described by Cirne et al. [25]. For such, a calibration curve was created for different concentrations of oil in n-hexane. The oil in each sample was extracted with n-hexane. An aliquot was placed in a cuvette and the content was analyzed.

For the experimental studies of the flotation kinetics with the pre-saturated affluent, the batch chamber shown in the schematic in Fig. 2 can be used. The flotation kinetics can be monitored with

the aid of measures of the reduction in the concentration of oil in the oily load of the chamber as a function of time by collecting samples from the base of the column and employing Eq. (1):

$$-\frac{dC_O}{dt} = k' C_O^n \quad (1)$$

in which:

C_O = concentration of oil

k' = kinetic oil removal constant

n = kinetic order of removal

Fractional oil removal (R) in relation to the oil mass in the affluent of the flotation chamber is given by:

$$R = \frac{C_{O_0} - C_O}{C_{O_0}} = 1 - \frac{C_O}{C_{O_0}} \quad (2)$$

in which C_{O_0} is the concentration of oil in the affluent of the batch-fed flotation chamber. Working algebraically to Eq. (2),

$$C_O = C_{O_0}(1 - R) \quad (3)$$

and introducing Eq. (3) into Eq. (1):

$$\frac{dR}{dt} = k' C_{O_0}^n (1 - R)^n \quad (4)$$

Assuming a constant k in place of the term $k' C_{O_0}^n$, we have a kinetic model (Eq. (5)) for the flotation of the pre-saturated effluent through the experimental determination of k and n:

$$\frac{dR}{dt} = k(1 - R)^n \quad (5)$$

Considering the similarity of an IPST to a battery of m mixture tanks, for removal kinetics of the order n, we have first-order oil removal kinetics (n = 1):

$$C_{O_m} = \frac{C_{O_0}}{(1 + k_1 \cdot \tau)^m} \quad (6)$$

in which:

C_{O_m} = concentration of oil in chamber m, mg L^{-1}

k_1 = kinetic oil removal constant for n = 1 order, min^{-1}

τ = mean fluid retention time of IPST, min

The product $k_1 t$ is identified as a dimensionless Damköhler number for first-order kinetics [7]. For second-order removal kinetics (n = 2), the calculation of the concentration at the output of chamber 2 gives:

$$C_{O_2} = \frac{C_{O_0} \pm \sqrt{1 + 4 \cdot k_2 \cdot \tau \cdot \left(\sqrt{\frac{-1 + 4 \cdot k_2 \cdot \tau \cdot C_{O_0}}{2 \cdot k_2 \cdot \tau}}\right)}}{2 \cdot k_2 \cdot \tau} \quad (7)$$

in which:

C_{O_2} = concentration of output in chamber m = 2, mg L^{-1}

k_2 = kinetic oil removal constant for n = 2 order, L mg^{-1} min^{-1}

In this case, the Damköhler number is represented by the product $\tau k_2 C_{O_0}$.

For n >2, it is not possible to use a general analytical expression and the concentration at the output of each stage has to be estimated stage by stage [26]. Thus, if the spatial time, initial concentration, number of stages and constant of the kinetic oil removal law are known, it is possible to estimate removal efficiency of a set of m floatation chambers operating with induced pre-saturation.

2.6. Analysis of kinetic data

For the determination of the kinetic constant of the flotation, batch experiments were performed using the installations of one of the stages of the bench-scale prototype (Fig. 3). For such, the steady-state operating conditions of the tower were initiated and interrupted with the simultaneous stopping of the microbubble pump and closure of the discharge valves of the selected chamber. Samples were removed every three minutes, giving rise to data for the creation of an oil concentration curve as a function of time.

The method for the creation of the kinetic curve was the adjustment of the variation in concentration over time (C_O) with the aid of a third-degree polynomial, as follows:

$$C_O = a + b \cdot t + c \cdot t^2 + d \cdot t^3 \quad (8)$$

in which:

t = time, min

a, b, c and d = constants of model

With the coefficients from Eq. (8), we can derive the expression and define the order of the kinetic law given by Eq. (9):

$$\frac{-dC_O}{dt} = k \cdot C_O^n \quad (9)$$

The kinetic constants of Eq. (9) can be estimated by adjusting the model through regression using the *Nonlinear Estimation* tool of Statistica (StatSoft®).

2.7. Statistical treatment of data

Significant differences between the oil and grease contents at the input and output of each stage of the tower were determined using one-way analysis of variance (ANOVA) with the aid of Statistica V.10 (StatSoft Inc., Tulsa, USA). Tukey's HSD test ($p < 0.05$) was used for comparisons when ANOVA revealed significant differences between samples [27]. Regarding the goodness of fit of the models that tested the first-order kinetic law for removal

Fig. 3. Bench-scale induced pre-saturation tower with different stages – Patent: BR 20 2017 016076 4.

efficiency, the quasi-Newton method was used as the numerical optimization in the regression of the data to find the most efficient solution among all possible solutions.

3. Results

Phenomenological models involving dimensional analysis have been developed to predict the efficiency of oil removal from water [28]. The determination of the removal efficiency of oil droplets dispersed in water in a DAF chamber is considered complex [29]. The kinetic behavior of a DAF chamber, which is also denominated a flotation reactor, is treated phenomenologically in two steps [29]. In a first region, known as the contact zone, the liquid interacts with air microbubbles, forming flocs. In a second region, known as the separation zone or clarification zone, the flocs are sent to the oily foam layer on the surface of the liquid in the chamber [30]. The authors cited proposed two kinetic models for the different behaviors of each region of the reactor. However, the strategy of generating microbubbles with a feed pump using the effluent itself transforms the floatation chamber into a means of oil droplet removal with a much simpler mechanism [31,7].

3.1. Continuous IPST prototype

Fig. 3 is a photograph of the IPST continuous prototype installed at the Prototype Lab of the Advanced Institute of Technology and Innovation (IATI, Recife, PE Brazil). The individual volume of each chamber was standardized at 3.4 L. After the installation of the equipment, preliminary experimental tests were performed for the definition of the operating characteristics of the IPST, using a synthetic effluent with a volumetric flow ranging from 0 to 0.040 $m^3\,h^{-1}$. The flow values for the pumps were adjusted with the aid of valves on the return pipes to the tanks.

3.2. Kinetic analysis of oil removal

Experiments were performed with and without the biosurfactant. Following the recommendations of Dhanarajan et al. [32], preliminary tests were performed using doses ranging from 250 mg L^{-1} to 500 mg L^{-1}, which determined that a content higher than 300 mg L^{-1} was not promising either technically or economically. Thus, the data displayed in Fig. 4 shows the effects of the addition and non-addition of the biosurfactant in the experimental arrangement shown in Fig. 2. The removal rate in both tests generated third-order polynomial models as a function of time. Table 1 displays the parameters of the regressions of the polynomials using the quasi-Newton numerical optimization method [33] for the addition and non-addition of the biosurfactant according to [8,17].

The R(t) polynomials were used to estimate the dR/dt values and the quasi-Newton numeric method was again used for the estimates of k and n in Eq. (6). Table 2 presents the kinetic constants found for Eq. (6) applied to the conditions of the addition and non-addition of the biosurfactant during the batch tests.

3.3. IPST operation diagrams

Two operation diagrams were obtained for the IPST by plotting dispersion graphs (Figs. 5 and 6), with the flow of the synthetic effluent (L h^{-1}) as the abscissa and microbubble flow (NL h^{-1}) and oil removal (%) as the ordinate. The IPST continuous prototype operated with three stages with and without the addition of the biosurfactant. The manometric height of the pumps was set at 6 bar according to Dassey and Theegala [34].

The two diagrams show the variation in oil removal under the operational conditions without (Fig. 5) and with (Fig. 6) the addition of the biosurfactant. The theoretical model for a battery of perfect-mixture reactors based on the kinetic analogy proposed by Walas [35] fit the experimental data, explaining more than 98 % of the variance. The behavior of the pre-saturation tower confirmed the increase in removal efficiency with the reduction in the flow and consequent increase in fluid retention time, that is, it was similar to the behavior of the oil–water separation flotation columns developed by Wang et al. [36] Xu et al. [37] and Gu and Chiang [38]. The highest removal efficiency values (97.0 % and 92.5 % for use and non-use of the biosurfactant, respectively) were achieved at approximately 10.2 min per stage according to Wang et al. [36]. The value of the output concentration with biosurfactant was of 22,5 mg L^{-1} and without biosurfactant was of 15 mg L^{-1}. The maximum amount of mineral oil tailings allowed by the Brazilian

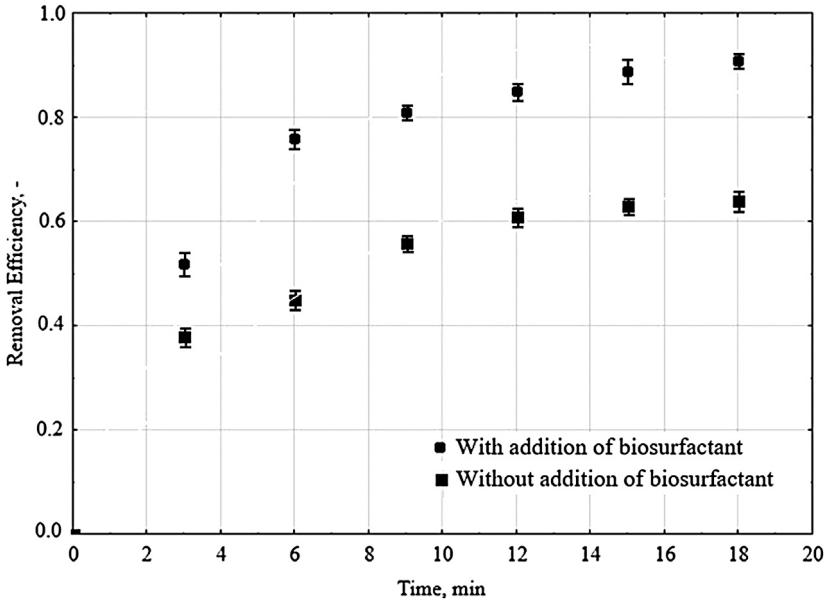

Fig. 4. Oil removal efficiency in bench-scale batch-fed flotation chamber as function of time with and without addition of biosurfactant (P = 1 atm, Temperature =28 °C, C_{O_0} = 300 mg L^{-1}).

Table 1
Parameter estimates by polynomial fit ($R = a + b \cdot t + c \cdot t^2 + d \cdot t^3$) with aid of quasi-Newton numerical method.

Condition	a	b	c	d	Variance explained (%)
With biosurfactant	0.011	0.210	−0.017	0.463e-3	99.5
Without biosurfactant	0.020	0.126	−0.009	0.237e-3	99.0

Table 2
Kinetic variables estimated with aid of nonlinear estimation using quasi-Newton method.

Condition	k	n	Variance explained (%)
With biosurfactant	0.022 min^{-1}	1	95.6
Without biosurfactant	0.131 $L\,g^{-1}\,min^{-1}$	2	95.0

Table 3
Experimental parameters with their ranges, intervals and uncertainties.

Parameter	Operating range	Interval	Uncertainty
Pressure	300–600	100	±3.0%
Input flow rates, Lh^{-1}	15–55	10	±2.2%
Air input flow rate, NL^{-1}	0–2.5	0.5	±2.5%
C_{O_0}, $mg\,L^{-1}$	300–500	–	±1.5%
Oil removal efficiency, %	40–100	10	±1.5%

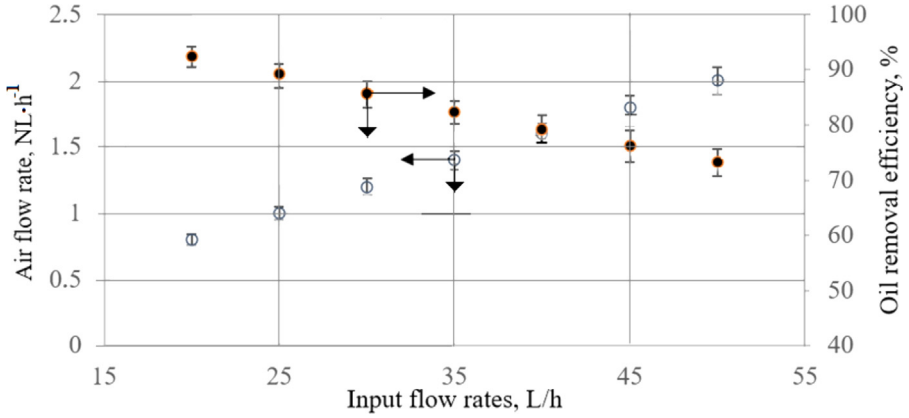

Fig. 5. IPST operation diagram without addition of biosurfactant (P = 1 atm, Temperature =28 °C, C_{O_0} = 300 mg L^{-1}).

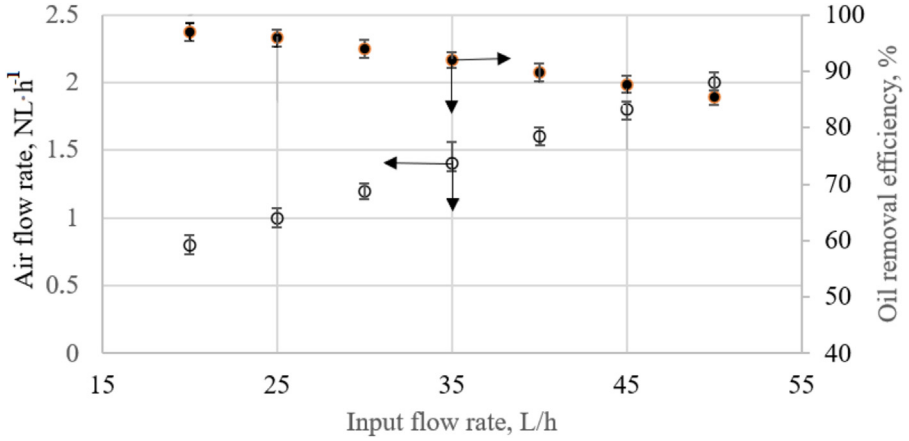

Fig. 6. IPST operation diagram with addition of biosurfactant (P = 1 atm, Temperature =28 °C, C_{O_0} = 300 mg L^{-1}).

Environmental Legislation (CONAMA) is of 20 mg L^{-1}. The biosurfactant produced by *Pseudomonas cepacia* CCT 6659 [8,17] was capable of reducing the surface tension of the medium from 65 mN m^{-1} to 26 mN m^{-1} to reduce the static Sauter diameters, increasing the efficiency of microbubbles production [39].

Table 3 indicates the range of the parameters in this study with their intervals and uncertainties. All the measurements were repeated for five times. The propagation of errors method was used to estimate the uncertainty of some parameters.

4. Conclusions

The induced pre-saturation tower with stages used for separation of mixture of water and semi-synthetic motor oil at 500 mg L^{-1} have shown that the addition of the biosurfactant produced by the bacterium *Pseudomonas cepacia* CCT 6659 led to an increase the oil removal efficiency from 92.5 % to 97.0 %, emphasizing that the oil removal efficiency was estimated with the aid of Damköhler numbers applied under the analogy of

considering the IPST to be a set of perfect-mixture tanks in series. The biosurfactant dosage associated with the centrifugal pump equipment for the generation of microbubbles in IPST Process increase the interfacial surface area which creates an environment for effective oil droplet-bubbles attachment. However, in this study, the IPST efficiency is directly proportional to the micro-bubble generation attributed to the centrifugal modified pump (500 kPa), input flow rate of oily water (20 L h^{-1}), air-water ratio (11.5 %) and hydraulic retention time (30.6 min). The value of the output concentration of oily water without using biosurfactant was of 22.5 mg L^{-1} and with using biosurfactant was of 15 mg L^{-1}, therefore, it is worth noting that the maximum amount of mineral oil tailings allowed by the Brazilian Environmental Legislation [40] is currently of 20 mg L^{-1}. The IPST Process for its innovation and efficiency can become a promising potential candidate in the treatment of oil-contaminated waters.

Declaration of Competing Interest

The authors declare that they have no known competing financial interests or personal relationships that could have appeared to influence the work reported in this paper.

Acknowledgments

This study was funded by the Research and Development Programme of the National Agency of Electrical Energy (ANEEL) and Thermoelectric EPASA (Centrais Elétricas da Paraíba), the Foundation for the Support of Science and Technology of the State of Pernambuco (FACEPE), the National Council for Scientific and Technological Development (CNPq), and the Coordination for the Advancement of Higher Education Personnel (CAPES – Finance Code 001). The authors are grateful to the Centre of Sciences and Technology of the Catholic University of Pernambuco and to the Advanced Institute of Technology and Innovation (IATI), Brazil.

References

[1] R. Etchepare, H. Oliveira, A. Azevedo, J. Rubio, Separation of emulsified crude oil in saline water by dissolved air flotation with micro and nanobubbles, Sep. Purif. Technol. 186 (2017) 326–332, doi:http://dx.doi.org/10.1016/j.seppur.2017.06.007.

[2] G. Huang, H. Xu, L. Wu, X. Li, W. Wang, Research of novel process route and scale-up based on oilwater separation flotation column, J. Water Reuse Desalin. (2017) 1–12.

[3] Y. Chi, J. Ma, J. Yang, Improved dissolved air flotation performances using chitosan under different dosing schemes, Pol. J. Environ. Stud. 26 (6) (2017) 2731–2737, doi:http://dx.doi.org/10.15244/pjoes/73806.

[4] J.M. Câmara, M.A. Sousa, E.B. Neto, M.C. Oliveira, Application of rhamnolipid biosurfactant produced by *Pseudomonas aeruginosa*in microbial-enhanced oil recovery (MEOR), J. Petrol. Explor. Prod. Technol. 1 (2019) 1–9, doi:http://dx.doi.org/10.1007/s13202-019-0633-x.

[5] H. She, D. Kong, Y. Li, Z. Hu, H. Guo, Recent advance of microbial enhanced oil recovery (MEOR) in China, Geofluids (2019) 1–15, doi:http://dx.doi.org/10.1155/2019/1871392 1871392.

[6] R.T. Rodrigues, J. Rubio, DAF – dissolved air flotation: potential applications in the mining and mineral processing industry, Int. J. Miner. Process. 82 (2007) 1–13 10.1016/j.minipro.2006.07.019.

[7] R.C.S. Henauth, R.S. Vasconcelos, A.E. Moura, L.A. Sarubbo, V.A. Santos, Microbubbles generation with aid of a centrifugal pump, Chem. Eng. Technol. (2016) 1–9, doi:http://dx.doi.org/10.1002/ceat.201500301.

[8] F.C.P. Rocha E Silva, N.M.P. Rocha E Silva, I.A. Silva, P.P.F. Brasileiro, J.M. Luna, R. D. Rufino, Santos, et al., Oil removal efficiency forecast of a Dissolved Air Flotation (DAF) reduced scale prototype using the dimensionless number of Damköhler, J. Water Process Eng. 23 (2018) 45–49, doi:http://dx.doi.org/10.1016/j.jwpe.2018.01.019.

[9] J.X. Zhang, Analysis on the effect of Venturi tube structural parameters on fluid flow, AIP Adv. 7 (2017)065315, doi:http://dx.doi.org/10.1063/1.4991441.

[10] H.J.B. Couto, M.V. Melo, G. Massaran, Treatment of milk industry effluent by dissolved air flotation, Braz. J. Chem. Eng. 21 (01) (2004) 83–91 ISSN 0104-6632.

[11] V. Camburn, V. Viswanatham, J. Linsev, D. Anderson, D. Jansen, et al., Design prototyping methods: state of the art in strategies, techniques, and guidelines, Des. Sci. 3 (2017) 1–33, doi:http://dx.doi.org/10.1017/dsj.2017.10.

[12] M.J. Chaprão, R.C.F. Soares da Silva, R.D. Rufino, J.L. Luna, V.A. Santos, L.A. Sarubbo, Formulation and application of a biosurfactant from *Bacillus methylotrophicus* as collector in the flotation of oily water in industrial environment, J. Biotecnol. 285 (2018) 15–22, doi:http://dx.doi.org/10.1016/j.jbiotec.2018.08.016.

[13] R.S. Vasconcelos, R.C.S. Henauth, A.E. Moura, V.A. Santos, L.A. Sarubbo, Strategy for a scale-up correlation in a Dissolved Air Flotation chamber, Chem. Eng. Technol. 38 (2015) 813–818, doi:http://dx.doi.org/10.1002/ceat.201400665.

[14] V.A. Santos, C.C. Dantas, E.A.O. Lima, S.B. Melo, Determination of the catalyst circulation rate in a FCC cold flow pilot unit using nuclear techniques, International Nuclear Atlantic Conference - INAC 2013 Recife, PE, Brazil, November 24–29, ASSOCIAÇÃO BRASILEIRA DE ENERGIA NUCLEAR, 2013 ABEN ISBN: 978-85-99141-05-2.

[15] V.A. Santos, C.C. Dantas, Transit time and RTD measurements by radioactive tracer to assess the riser flow pattern, Powder Technol. 140 (2004) 116–121, doi:http://dx.doi.org/10.1016/j.powtec.2004.01.005.

[16] A. Ramya, S. Vanapalli, 3d printing technologies in: various applications, Int. J. Mech. Eng. Technol. 7 (3) (2016) 396–409. http://www.iaeme.com/currentissue.asp?JType=IJMET&VType=7&IType=3.

[17] F.C.P. Rocha E Silva, N.M.P. Rocha E Silva, I.A. Silva, J.M. Luna, R.D. Rufino, et al., Dissolved air flotation combined to biosurfactants: a clean and efficient alternative to treat industrial oily water, Rev. Environ. Sci. Biotechnol. 17 (4) (2018) 591–602, doi:http://dx.doi.org/10.1007/s11157-018-9477-y.

[18] M. Han, Y. Park, J. Lee, J. Shim, Effect of pressure on bubble size in dissolved air flotation, Water Supply 2 (5–6) (2002) 41–46, doi:http://dx.doi.org/10.2166/ws.2002.0148.

[19] R.A. Galdino, A.E. Moura, V.A. Santos, L.A. Sarubbo, Strategy for controlling the level in a Dissolved Air Flotation chamber, J. Chem. Chem. Eng. 9 (2015) 344–352, doi:http://dx.doi.org/10.17265/1934-7375/2015.05.006.

[20] H.J. Yan, Y. Chen, X.Y. Chu, Y. Chu, Effect of structural optimization on performance of Venturi injector, Earth Environ. Sci. 15 (2012) 1–8, doi:http://dx.doi.org/10.1088/1755-1315/15/7/072014.

[21] R.C. Hibeller, Fluid Mechanics, first edition, Pearson Prentice Hall, Malaysia, 2017, pp. 840 ISBN 10: 1-292-08935-0.

[22] R.C.F. Soares da Silva, D.G. Almeida, H.M. Meira, E.J. Silva, C.B.B. Farias, R.D. Rufino, J.M. Luna, L.A. Sarubbo, Production and characterization of a new biosurfactant from *Pseudomonas cepacia* grown in low-cost fermentative medium and its application in the oil industry, Biocatal. Agric. Biotechnol. 12 (2017) 206–215, doi:http://dx.doi.org/10.1016/j.bcab.2017.09.004.

[23] I. Langmuir, The constitution and fundamental properties of solids and liquids. II. Liquids, J. Am. Chem. Soc. 39 (1917) 1848–1906, doi:http://dx.doi.org/10.1021/ja02254a006.

[24] F.C.P. Rocha e Silva, N.M.P. Rocha E Silva Moura, Alex Elton de Moura, R.A. Galdino, J.M. Luna, R.D. Rufino, V.A. Santos, L.A. Sarubbo, Effect of biosurfactant addition in a pilot scale Dissolved Air Flotation system, Sep. Sci. Technol. 50 (2015) 618–625, doi:http://dx.doi.org/10.1080/01496395.2014.957319.

[25] I. Cirne, J. Boaventura, Y. Guedes, E. Lucas, Methods for determination of oil and grease contents in wastewater from the petroleum industry, Chem. Chem. Technol. 10 (2016) 4.

[26] B.L. Crynes, H.S. Fogler, AIChEMI Moduat Instruction: Series E, Kinectics - Rate of Reaction, Sensitivity, and Chemical Equilibrium, AIChE, New York, 1981, pp. 94.

[27] E. Ostertagová, O. Ostertag, Methodology and application of one-way ANOVA, Am. J. Mech. Eng. 1 (7) (2013) 256–261, doi:http://dx.doi.org/10.12691/ajme-1-7-21.

[28] A.M.R. Radzuan, M.A. Abia-Biteo Belope, R.B. Thorpe, Removal of fine oil droplets from oil-in-water mixtures by dissolved air flotation, Chem. Eng. Res. Des. 115 (2016) 19–33, doi:http://dx.doi.org/10.1016/j.cherd.2016.09.013.

[29] J. Haarhoff, J.K. Edzwald, Modelling of floc-bubble aggregate rise rates in dissolved air flotation, Water Sci. Technol. 43 (8) (2001) 175–184, doi:http://dx.doi.org/10.2166/wst.2001.0492.

[30] J. Behin, S. Bahrami, Modeling an industrial dissolved air flotation tank used for separating oil from wastewater, Chem. Eng. Process. Processe Intensification 59 (2012) 1–8, doi:http://dx.doi.org/10.1016/j.cep.2012.05.004.

[31] P.P.F. Brasileiro, L.B. Santos, M.J. Chaprão, D.G. Almeida, R.C.F. Soares da Silva, B. A.S. Roque, V.A. Santos, L.A. Sarubbo, M. Benachour, Construction of a microbubble generation and measurement unit for use in flotation systems, Chem. Eng. Res. Des. 153 (2020) 212–219, doi:http://dx.doi.org/10.1016/j.cherd.2019.10.028.

[32] G. Dhanarajana, P. Perveena, A. Royb, S. Deb, R. Sena, Performance Evaluation of Biosurfactant Stabilized Microbubbles in Enhanced Oil Recovery Disponível em: https://www.biorxiv.org/content/10.1101/504431v1.full.pdf, acesso em 21/10/2019, (2018) .

[33] R.L. Burden, J.D. Faires, Numerical Analysis, Brooks/Cole, USA, 2011.

[34] A. Dassey, C. Theegala, Optimizing the air dissolution parameters in an unpacked dissolved air flotation system, Water 4 (2012) 1–11, doi:http://dx.doi.org/10.3390/w4010001.

[35] S.M. Walas, Reaction Kinetics for Chemical Engineers, Butterworth, Boston, 1989.

[36] C. Wang, Z. Wang, X. Wei, X. Li, A numerical study and flotation experiments of bicyclone column flotation for treating of produced water from ASP flooding, J. Water Process Eng. 32 (2019)100972, doi:http://dx.doi.org/10.1016/j.jwpe.2019.100972.

[37] H. Xu, J. Liu, Y. Wang, G. Cheng, X. Deng, X. Li, Oil removing efficiency in oil–water separation flotation column, Desalin. Water Treat. 53 (2015) 2456–2463, doi:http://dx.doi.org/10.1080/19443994.2014.908413.

[38] X. Gu, S.H. Chiang, A novel flotation column for oily water cleanup, Sep. Purif. Technol. 16 (1999) 193–203.
[39] P.P.F. Brasileiro, R.C.F. Soares da Silvad, B.A.S. Roque, V.A. Santosc, L.A. Sarubbo, M. Benachour, Efficiency of microbubble production using surfactants for the treatment of oily water by flotation, Chem. Eng. Res. Des. 168 (2021) 254–263, doi:http://dx.doi.org/10.1016/j.cherd.2021.02.015.
[40] BRASIL Ministério do Meio Ambiente, Conselho Nacional de Meio Ambiente (CONAMA), Dispõe sobre a classificaçao dos corpos de a'gua e diretrizes ambientais para o seu enquadramento, bem como estabelece as condiçoes e padrões de lançamento de efluentes, e da' outras providências, Diário Oficial da República Federativa do Brasil, Brasília, 2005, pp. 58–63 Resolução nº 357, de 17 de março de. 18 mar. Seção 1.